Corneal Stroma Cell Density Evolution in Keratoconus Corneas Following the Implantation of Adipose Mesenchymal Stem Cells and Corneal Laminas: An In Vivo Confocal Microscopy Study

Mona El Zarif,[1,3,7,8] Karim A. Jawad,[1] Jorge L. Alió Del Barrio,[2,3] Ziad A. Jawad,[1] Antonio Palazón-Bru,[4] María P. de Miguel,[5] Peggy Saba,[6] Nehman Makdissy,[7] and Jorge L. Alió[2,3]

[1]Optica General, Saida, Lebanon
[2]Cornea, Cataract and Refractive Surgery Unit, Vissum Corporación, Alicante, Spain
[3]Division of Ophthalmology, Miguel Hernández University, Alicante, Spain
[4]Department of Clinical Medicine, Miguel Hernández University, Alicante, Spain
[5]Cell Engineering Laboratory, IdiPAZ, La Paz Hospital Research Institute, Madrid, Spain
[6]Institut Technique Industriel Superieur Dekwaneh, Beirut, Lebanon
[7]Genomic Surveillance and Biotherapy Laboratory, Faculty of Sciences, Lebanese University, Tripoli, Lebanon
[8]Doctoral School of Sciences and Technology, Lebanese University, Hadath, Lebanon

Correspondence: Jorge L. Alió, Vissum, Calle Cabañal, 1. 03016 Alicante, Spain; jlalio@vissum.com.

Received: November 15, 2019
Accepted: February 26, 2020
Published: April 17, 2020

Citation: El Zarif M, A. Jawad K, Alió Del Barrio JL, et al. Corneal stroma cell density evolution in keratoconus corneas following the implantation of adipose mesenchymal stem cells and corneal laminas: an in vivo confocal microscopy study. *Invest Ophthalmol Vis Sci.* 2020;61(4):22. https://doi.org/10.1167/iovs.61.4.22

Purpose. To report the corneal stroma cell density evolution identified by in vivo corneal confocal microscopy in humans using injected autologous adipose-derived adult stem cells (ADASCs) and corneal decellularized laminas in corneas with advanced keratoconus.

Methods. Interventional prospective, consecutive, randomized, comparative series of cases. A total of 14 keratoconic patients were randomly distributed into three groups for three types of surgical interventions: group 1 (G-1), autologous ADASC implantation (n = 5); group 2 (G-2), decellularized human corneal stroma (n = 5); and group 3 (G-3), autologous ADASCs + decellularized human corneal stroma (n = 4).

Results. A gradual and significant increase ($P < 0.001$) was observed in the cellularity in the anterior and posterior stroma of patients in G-1, G-2, and G-3 a year after the surgery in comparison with the preoperative density level. The same result was observed at the mid-corneal stroma in G-1 and at the anterior and posterior surfaces and within the laminas in G-2 and G-3. The cell density of patients receiving ADASC recellularized laminas (G-3) was statistically significantly higher ($P = 0.011$) at the anterior surface and within the lamina ($P = 0.029$) and at the posterior surface than in those implanted only with decellularized laminas (G-2).

Conclusions. A significant increase in cell density occurred up to 1 postoperative year at the corneal stroma following the implantation of ADASCs alone, as well as in those cases implanted with decellularized and recellularized laminas at the different levels of the analysis. However, this increase was significantly higher in the ADASC recellularized laminas.

Keywords: corneal confocal microscopy, keratocytes, keratoconus, autologous adipose-derived adult stem cells, corneal stem cell therapy

Keratoconus is the most frequent and prevalent type of corneal dystrophy.[1,2] It consists of a progressive loss of corneal strength,[3] associated with a gradual loss of the stromal keratocytes. The number of keratocytes decreases from the anterior to posterior stroma,[4] and there is a progressive thinning of the corneal stroma,[4,5] even though some phenotypic differences in the expression of the disease are present.[6] However, in all cases, a loss of keratocyte density, apoptosis, and a loss of corneal stroma occur over time,[4,7–8] with corneal deformation and a shift in the location of the corneal apex[9] leading to progressive visual loss.[6] The disease still has an unclear genomic profile.[10] In keratoconus, the use of noninvasive diagnostic methods, such as confocal microscopy, has recently provided relevant information about the microanatomical changes that happen during the evolution of the disease.[4,11]

The visual loss that keratoconus patients suffer is treated in different ways, ranging from contact lenses that reduce the higher order aberrations and mask the irregular astigmatism[12] to surgical options, with variable success[13]; however, none of these procedures has yet addressed regeneration of the diseased corneal tissue. Recently, we proposed the

clinical use of acellular corneal tissue, with or without autologous stem cell repopulation, to increase the corneal thickness and to promote the production of new collagen, aiming to improve the biological and clinical condition of the keratoconic cornea and halting the progression of the disease.[14–19] Based on these reports, the use of mesenchymal stem cells such as autologous adipose-derived adult stem cells (ADASCs) or corneal stroma decellularized laminas with or without ADASC recellularization implanted in the corneal stroma has become a promising therapeutic option for keratoconus treatment.

We report herein the results of our evaluation of the evolution of corneal stroma cellularity, studied with corneal confocal microscopy, in eyes that have been the subject of corneal regeneration experiences.[14–16] The visual and refractive results from the interim analyses of this cohort performed by our group at 6 and 12 months have been reported in previous publications.[14–16] Here, we report the changes induced in the cellularity and distribution of corneal cells following implantation of ADASCs, alone or via decellularized laminas as carriers, after 1 year of follow-up.

Methods

Study Design and Patients

This study was an interventional, prospective, randomized clinical investigation of 14 consecutive advanced keratoconus patients. The study was conducted in strict adherence to the tenets of the Declaration of Helsinki. The ethical committee of the institutional review board of the Reviva Research and Application Center approved this study (ClinicalTrials.gov number NCT02932852). All study patients signed an adequate consent form prior to the surgical procedure. All patients were randomly distributed into three study groups:

Group 1 (G-1)—Autologous ADASC implantation (five patients, two females and three males; ages ranging from 23 to 43 years with an average age of 32.2).
Group 2 (G-2)—Decellularized human corneal stroma transplantation (five patients, four females and one male; ages ranging from 25 to 43 years with an average age of 32.4).
Group 3 (G-3)—Autologous ADASC + decellularized human corneal stroma transplantation (four patients, three females and one male; ages ranging from 30 to 49 years with an average age of 36.25).

The inclusion and exclusion criteria of the study have been defined in our previous publications on this clinical study.[14–16]

Surgical Procedure

Autologous ADASC Implantation. Topical anesthesia was used, and a 60-kHz IntraLase iFS femtosecond laser (Abbott Medical Optics, Inc., Irvine, CA, USA) was utilized in single-pass mode for the recipient corneal lamellar dissection. An intrastromal laminar cut 9.5 mm in diameter was created mid-depth in the thinnest preoperative pachymetry point measured by anterior segment optical coherence tomography (OCT) (Visante OCT; Carl Zeiss Meditec, Jena, Germany). A 30° anterior side-cut incision was made. The corneal intrastromal pocket was opened with a Morlet lamellar dissector (Duckworth & Kent, Baldock, UK). Then, with a 25-gauge cannula, 3 million autologous ADASCs contained in 1 ml of PBS were injected into the pocket (Fig. 1). To reduce intraocular pressure and allow a larger volume of cells to be injected into the stroma pocket, a 1-mm corneal paracentesis was performed. Topical antibiotics and steroids (Tobradex; Alcon, Geneva, Switzerland) were applied at the end of the surgery. No corneal sutures were used.[14,16]

Lenticule Implantation. Topical anesthesia was applied with oral sedation for all surgeries. The IntraLase iFS femtosecond laser was used to perform the same stromal dissection but with a 50° anterior side cut. After opening the corneal intrastromal pocket, the lamina was inserted, centered, and unfolded through gentle tapping and massage from the epithelial surface of the host (Fig. 2). As before, a temporary limbal paracentesis was performed to reduce the intraocular pressure. In those cases that received recellularized laminas (G-3), to compensate for the cellular damage expected by the implantation process, the pocket was irrigated, immediately before and after the lamina insertion, with a solution containing an additional 1 million autologous ADASCs in 1 ml of PBS with a 25-gauge cannula (Figs. 2E–2H). The incision was then closed with an interrupted 10/0 nylon suture that was removed 1 week after the operation. Topical antibiotics and steroids (Alcon Tobradex) were applied at the end of the surgery.[15,16]

All surgeries were performed by the same surgeons (J.L.A. and J.L.A.B.) at the Laser Vision Center (Beirut, Lebanon).

In Vivo Confocal Microscope Device

A HRT3 confocal microscope with a Rostock Cornea Module (RCM) (Heidelberg Engineering, Heidelberg, Germany) was used. The light source of this confocal microscope is a coherent type of diode laser, with a wavelength of 670 nm and a minimum resolution of 1024 × 768 (16 bit).[20] Coherent light was used to improve the contrast and quality of the images of the corneal stroma, particularly the cells.[4]

Use of the Corneal Microscope. A signed informed consent was obtained from patients for the confocal microscopy study. A drop of topical anesthetic (oxybuprocaine 0.4%) was applied in the eye to be examined. The confocal microscope was set at +12 D. A drop of a high-viscosity gel (2.0 mg/g of carbomer) was applied to the front surface of the microscope lens of the RCM. Then, a RCM TomoCap was placed on top of the RCM objective. A drop of the same viscous gel was also applied on the upper part of the outer surface of the TomoCap and in the patient's eye to be examined. The patient was placed in a stable and comfortable position, with the eye aligned with the lens of the confocal microscope, and was instructed to keep looking at the light inside the lens. The focal position was reset to 0 at the superficial epithelial cells of the examined eye. The RCM was then turned clockwise or anticlockwise 0 ± 50 μm, and the focal plane was adjusted to the desired cell layer. Finally, at least four images were obtained for every 50 μm of depth and stored following a previously described protocol.[20] The images analyzed in this study were indeed at different stromal depths but always belonged to a central diameter ≤ 9 mm and were below the measurement of the intrastromal diameter pocket.[14–16]

Method of Stromal Cell Counting. Images that had a better quality of contrast and illumination were selected from the images captured and stored during the experience.

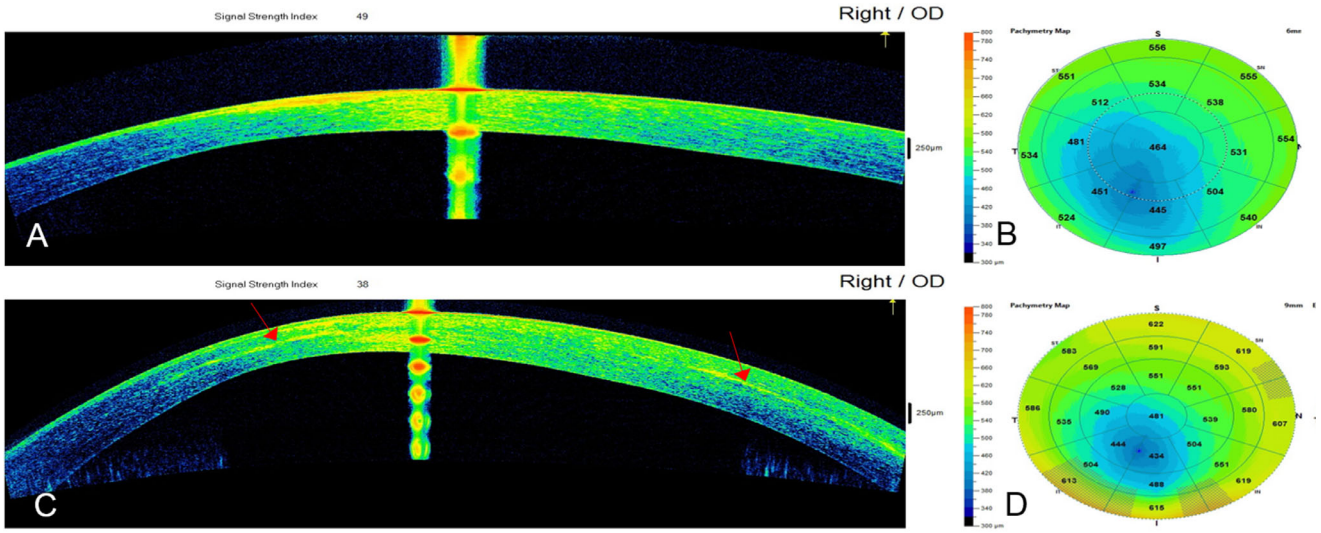

Figure 1. Cornea Visante OCT images and pachymetric maps for case 2 from G-1. (**A**, **B**) Preoperative examination, and (**C**, **D**) 12 months after surgery. Observe the patchy hyperreflective areas (red arrows) at the level of the stromal pocket compatible with areas of new collagen production. The distribution of these areas was not homogeneous along the surgical plane.

An area known as a region of interest (ROI) was determined, and the same ROI (0.1000 mm^2) was used for all cell counts in all layers of the corneal stroma.[4,20] The morphology criteria used in the present study to differentiate the corneal stroma cells from the inflammatory cells are described below.

We used 50% brightness and contrast (Fig. 3A) for all images. Cells that were more illuminated and more refringent[7,8] were selected and marked in blue.[20] These cells were white or light gray in color and had clear and well-defined edges.[4] Dark gray cells were not taken into consideration, as they did not belong to the chosen 50-µm plane. The confocal cellular brightness is attributed to the nuclear content of these cells.[4,7,11,14–16,21,22] Because of their irregular oval-shaped bodies,[7] differences in brightness among them can be attributed to different metabolic activation and direction of incidence of the laser beam.[7] Only the cell nuclei that were identified with the method mentioned above were defined as corneal stromal cells and included in the cell counting process. For simplification throughout the paper, when we talk about cell density or morphology, we are referring to the density or morphology of the cell nucleus and not the cell membrane that was observed by confocal microscopy.[4,7,11,14–16,21,22]

The highly reflective material was not considered in the cell count whenever the size of the reflective morphology exceeded the size that we considered similar to stromal keratocyte, whether in normal or in keratoconic corneas.[4,7,11,14–16,21,22] For this reason, we have considered that this structure corresponds to a fibrotic material.

After the first count was performed, the contrast was increased to the maximum and the brightness decreased to the minimum. Any stromal cell that disappeared from the chosen plane was eliminated, and only those cells that remained were used for the final cell count, even if they were faintly identified in the image (Fig. 3B).

ADASC Cell Counting. The counting method for transplanted ADASCs was performed in a similar way. ADASCs appear rounded in shape, voluminous, and refringent (Fig. 4A).[14] The morphology and evolution of the ADASCs over time are described later in the Results section (Fig. 4B).

Cell Count on Decellularized and Recellularized Laminas. When the decellularized (G-2) and recellularized (G-3) laminas appeared without well-defined cell structures, they were considered totally acellular in the 0.1-mm^2 area that we delimited in our study (Fig. 5A).[15,16] All structures that appeared on the anterior surface, on the posterior surface, or in the mid-stroma of the lamina; that showed well-defined edges that were white or light gray in color; and that had a morphology similar to that of a keratocyte nucleus were counted as a cell (Figs. 5B, 5C, 6).

Corneal Cell Density Calculation. To obtain the cellular density, we first defined the ROI (mm^2)[20] and then proceeded to count the cells with the methodology described above. The cellular density for the chosen area was calculated by the confocal microscope software as the number of cells multiplied by 10 cells/mm^2 ± SD.[8,20]

To calculate the cell density of the corneal stroma among the three groups, we divided the measurements of the stroma into three zones: anterior, mid-, and posterior stroma. The mid-stroma coincided with the surgical plane (calculated as half of the thinnest point of the cornea obtained by OCT ± 50 µm).[14–16] The anterior stroma is the stroma located below Bowman's membrane, and the posterior stroma is the stroma located above Descemet's membrane.[14–16] For those measurements where a lamina was present (postoperative G-2 and G-3), we divided the lamina into three areas: anterior surface, lamina posterior surface, and lamina mid-stroma (Fig. 6F)

The main outcome measures of this study are the changes in and evolution of corneal stroma cellular density over a 1-year follow-up period, as analyzed using corneal confocal microscopy. Cellular density was studied before surgery and at 1, 3, 6, and 12 months after surgery. Preoperative cellular density was measured in the anterior, mid-, and posterior stroma in G-1, as well as in G-2 and G-3. Postoperative cellular density in G-2 and G-3 was studied in the anterior and

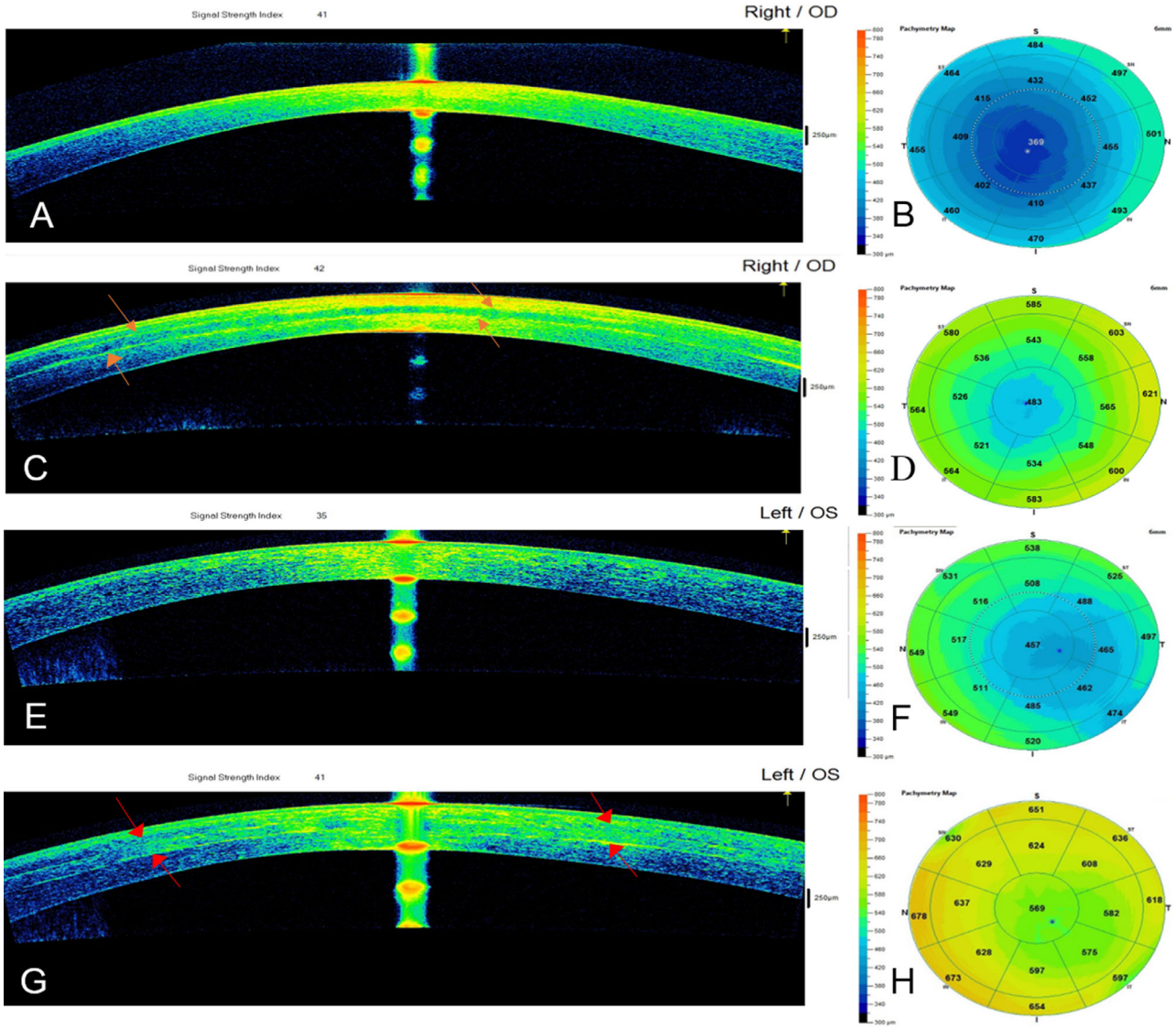

Figure 2. Cornea OCT images and pachymetric maps for case 5 from G-2: (**A**) Preoperative OCT examination, (**B**) preoperative pachymetric map, (**C**) 12-month postoperative OCT (red arrows represent the graft edges), and (**D**) significant improvement in the pachymetric map 12 months after surgery. Cornea OCT images and pachymetric maps for case 10 from G-3: (**E**) preoperative OCT examination, (**F**) preoperative pachymetric map, (**G**) 12-month postoperative OCT (red arrows represent the graft edges), and (**H**) significant improvement in the pachymetric map 12 months after surgery.

posterior stroma and through the lamina, with the purpose of exploring the evolution of its cellular component during the study time.

Statistical Analysis

Statistical analysis was performed by generalized linear mixed models with a Poisson variable as an outcome (fixed effects, time and group; random effects, individual). This Poisson variable corresponded to the keratocyte nuclei densities (Poisson distribution), indicating the means of cell nuclei appearing in the captured figures at different levels of the corneal stroma (anterior, intermediate, and posterior) or on the anterior surface, mid-stroma, and posterior surface of the implanted tissue for the studied time intervals. A Poisson variable, unlike one that follows in a normal distribution, is expressed by a single parameter, which is the average number of events only (Figs. 7, 8). The standard deviation of the Poisson variable (generally known as lambda) is not shown in the figures, but it is the same as the average parameter, as compared to a normal distribution which is expressed by mean and standard deviation. On the other hand, this average parameter (obtained through mixed generalized linear models) takes into account all of the measurements of all of the individuals and assesses the variability between individuals and within them. Consequently, the results presented here are at the group level and provide all of the information necessary to understand the impact of the intervention. Scatterplots were developed to help interpret the results, and the goodness of fit of the models was obtained through the likelihood ratio test. The type I error significance

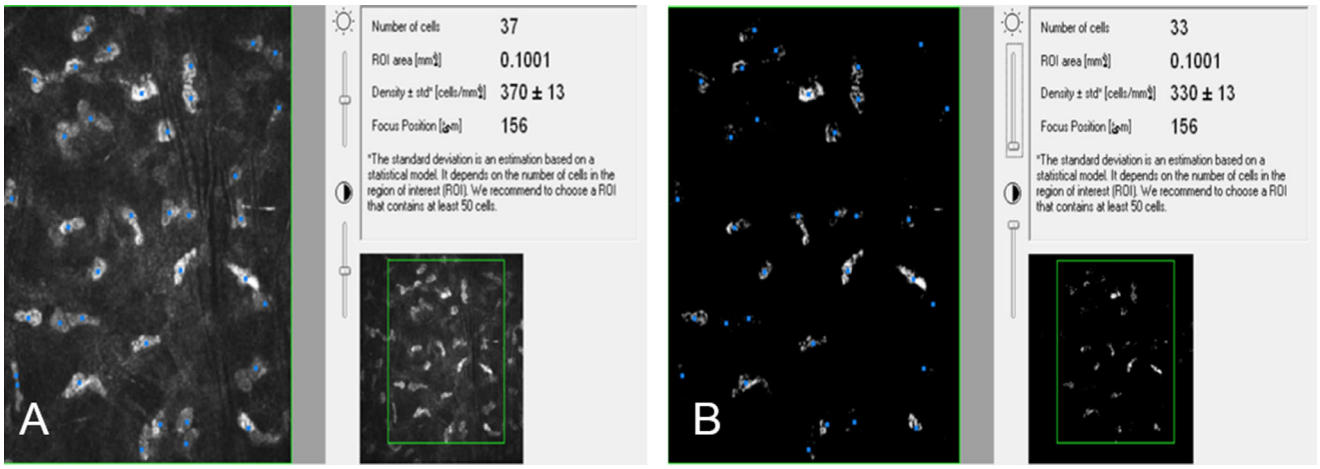

Figure 3. (**A**) Cell count performed with medium brightness and contrast. The more illuminated and more refringent cells were counted, and the keratocytes are marked in blue. (**B**) Elimination of keratocytes that do not belong to the plane under observation is possible using low brightness and high contrast settings.

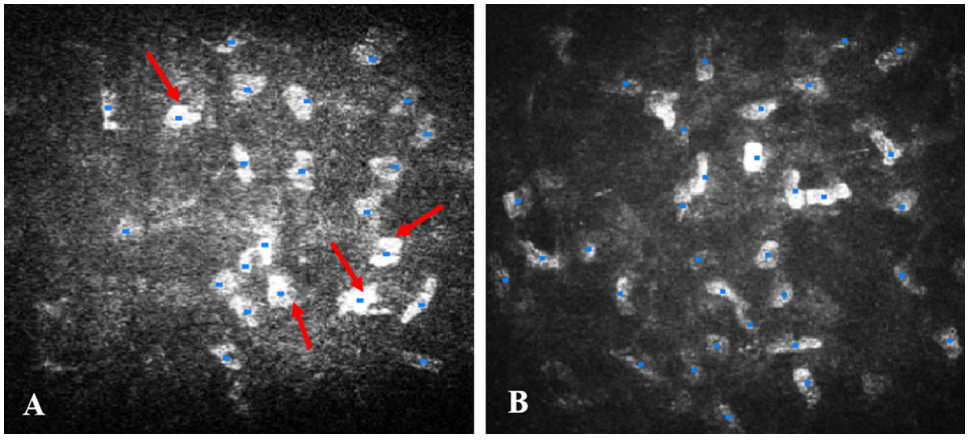

Figure 4. ADASC counting in G-1. (A) Count of ADASCs (red arrows) and keratocytes 1 month following surgery of a keratoconic patient; the cells are marked in blue. The ADASCs have a rounded shape and are larger, more luminous, and more refringent than the normal keratocytes. (**B**) Cell count of a keratoconic patient 1 year after implantation of ADASCs; all corneal stroma cells demonstrate a similar shape.

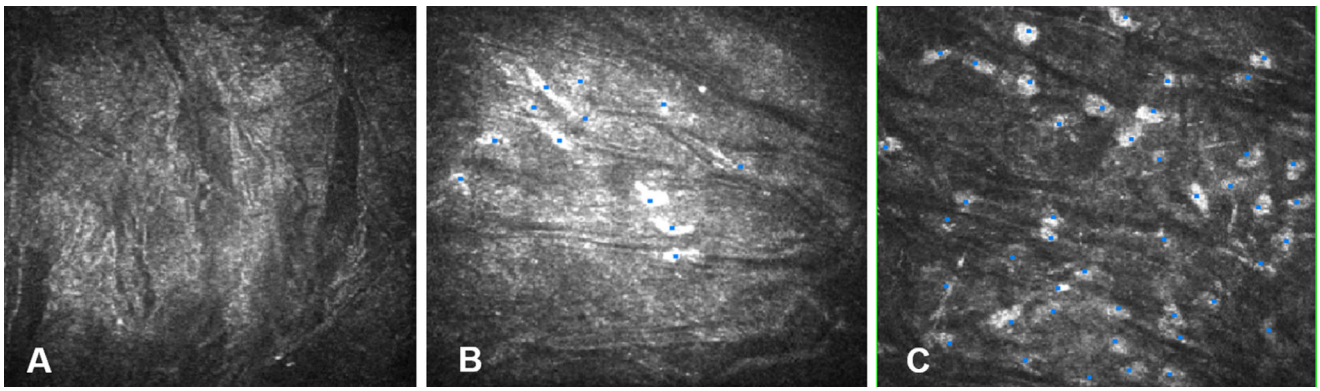

Figure 5. Cell count on decellularized laminas for case 9 from G-2. (**A**) Anterior surface of a decellularized lamina that appears without cells 1 month after surgery. (**B**) Cell count on the posterior surface of a lamina 3 months after surgery. Cells show different morphology from the host corneal stromal cells. These cells are smaller. (**C**) Cell count on the posterior surface of a lamina 1 year after surgery. All cells demonstrate a morphology identical to that of normal corneal stromal keratocytes.

Investigative Ophthalmology & Visual Science

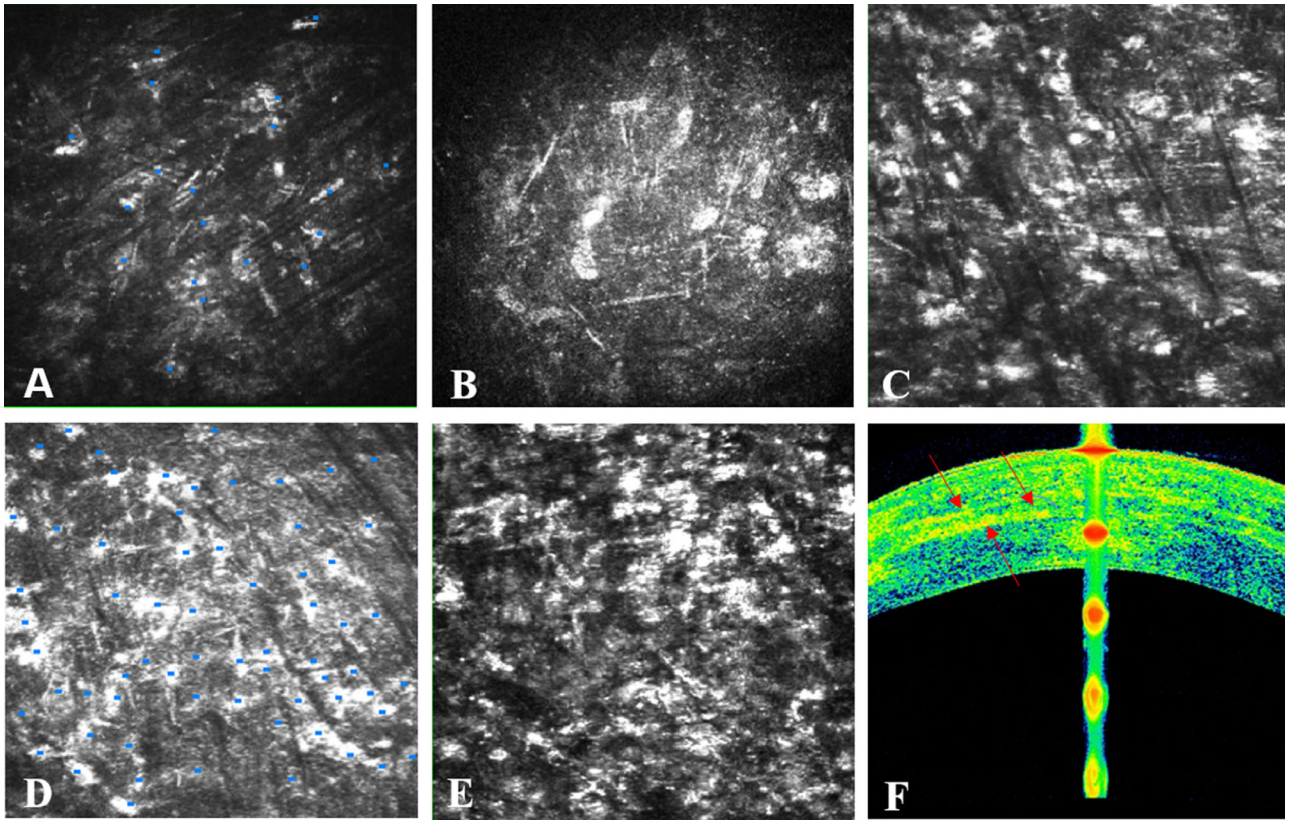

Figure 6. Cell count on recellularized lamina for case 13 from G-3. (**A**) Anterior surface of a recellularized lamina 1 month after the operation; few ADASCs can be seen (marked in blue). (**B**) Posterior surface of the recellularized lamina 1 month after the operation; note the presence of a few ADASCs similar in morphology to keratocytes. (**C**) Anterior surface of the recellularized lamina 12 months after surgery showing an abundant number of stromal cells. (**D**) Mid-stroma of the lamina 12 months after surgery showing a high number of stromal cells. (**E**) Posterior surface of the recellularized lamina 12 months after surgery showing a high number of stromal cells. (**F**) OCT image where the red arrows represent the anterior and posterior surfaces, as well as the mid-stroma, of the recellularized lamina 12 months after surgery.

level was set at 0.05, and the statistical software we used was R 3.5.1.

The maximum number of images for each patient was collected to calculate cell density. To not alter the results, mathematical models of repeated measures were used to control the variability of each individual.

We considered the average cell counts of two observers who performed them separately following the same scientific standards; when there was a discrepancy between them of more than 20%, the count was repeated or other images were taken, if possible, until achieving agreement.

Results

Patients Implanted with ADASCs Alone (G-1)

Morphological Results. Implanted ADASCs could be seen in clusters 1 to 3 months following the implantation surgery. The ADASCs appeared to be rounded in shape, more luminous, more refringent, compared with the host keratocytes (Fig. 2A).[14,16] However, the shape of the ADASCs changed from round to fusiform 6 months after the implantation.[14,16] The morphological differences between the ADASCs and host keratocytes disappeared over time (Fig. 4B).

Cell Density Results. Twelve months after implantation, we observed a gradual, statistically significant increase ($P < 0.001$) in the cellular density at the anterior, mid-, and posterior stroma (Fig. 7).

Patients Implanted with Decellularized Corneal Laminas (G-2)

Morphological Results. One month after surgery, the decellularized lamina appeared acellular (Fig. 5A). Three months after surgery, the patient's host cells began to colonize the lamina, progressively increasing in number over time (Figs. 5B, 8). These cells differed in morphology from the native keratocytes of the cornea, as they appeared smaller and less voluminous (Fig. 5B). The shape of these cells at 6 months became more similar to the usual keratocytes of the corneal stroma,[15] before fully developing into cells that had an identical morphology to the normal keratocytes 1 year after surgery (Fig. 5C).[16]

Cell Density Results. One month after surgery, the transplanted laminas generally remained acellular in most of the patients (Fig. 5A).[15,16] We observed means of 31 cells/mm^2 in the anterior surface of the lamina, 17 cells/mm^2 within the lamina, and 48 cells/mm^2 in the posterior surface of the lamina (Fig. 8). Cell density increased over time (Figs. 5B, 8). We observed that

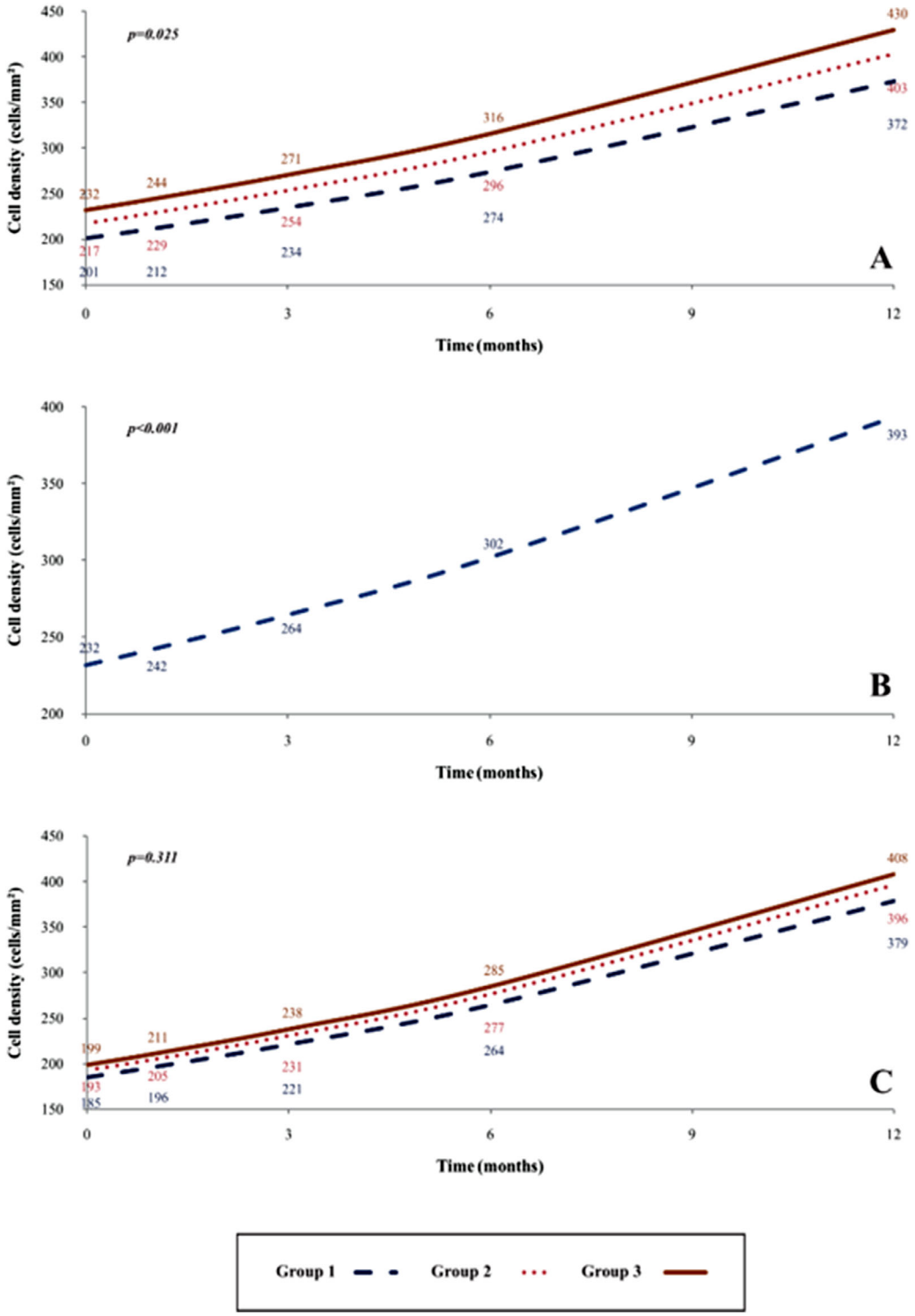

Figure 7. Cellular density change in the corneal stroma of G-1, G-2, and G-3. (A) Increase in cell density over time in the anterior stroma of the cornea in G-1, G-2, and G-3 from the preoperative period until 12 months after surgery. A significant statistical difference ($P = 0.025$) among the groups was detected. (B) Statistically significant increase in cell density ($P < 0.001$) over time in the mid-stroma of the cornea in G-1 from the preoperative period until 12 months after surgery. (C) Increase in cell density over time in the posterior stroma of the cornea in G-1, G-2, and G-3 from the preoperative period until 12 months after surgery. There was no significant difference among the three groups ($P = 0.311$).

recellularization began on the posterior surface of the lamina, followed by on the anterior surface and within the lamina (Fig. 8). Moreover, 1 year after implantation, the anterior, mid-, and posterior surfaces of the laminas were more colonized by keratocyte-type cells (Fig. 5C),[16] until reaching statistically significant values ($P < 0.001$) 12 months

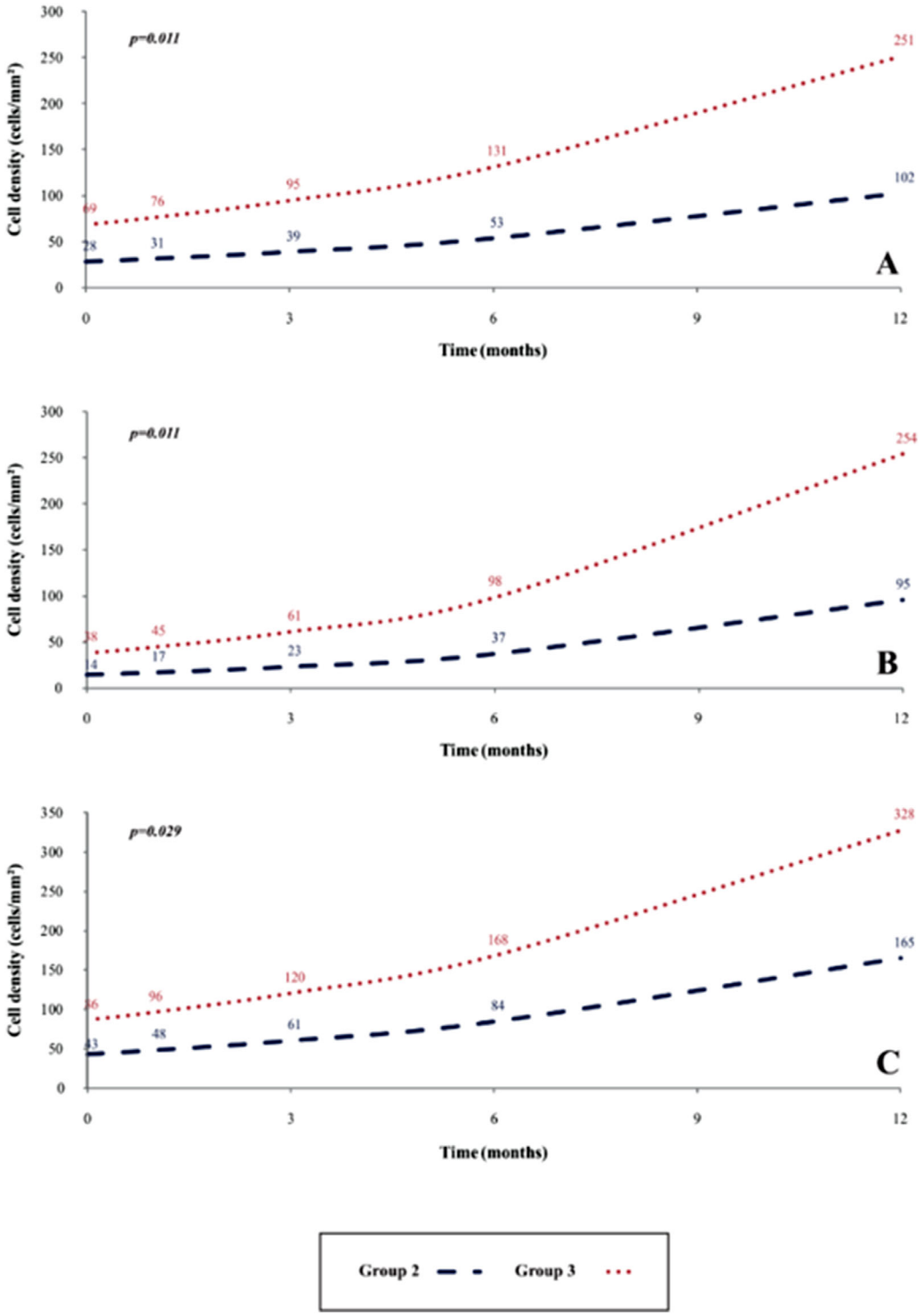

Figure 8. Cellular density change in the anterior and posterior surfaces of the lamina, as well as the mid-stroma of the lamina. (A) Increase in cell density over time in the anterior surface of the lamina in G-2 and G-3 from the preoperative period until 12 months after surgery. A significant statistical difference ($P = 0.011$) exists between G-2 and G-3. (B) Increase in cell density over time in the mid-stroma of the lamina in G-2 and G-3 from the preoperative period until 12 months after surgery. A significant statistical difference ($P = 0.011$) between G-2 and G-3 was detected. (C) Increase in cell density over time in the posterior surface of the lamina in G-2 and G-3 from the preoperative period until 12 months after surgery. A significant statistical difference ($P = 0.029$) between G-2 and G-3 was detected.

after surgery in comparison to the first postoperative month (Fig. 8). The keratocyte density 12 months after surgery in the anterior and posterior stroma increased, as well, in a statistically significant manner compared with preoperative values ($P < 0.001$) (Figs. 7A, 7C).

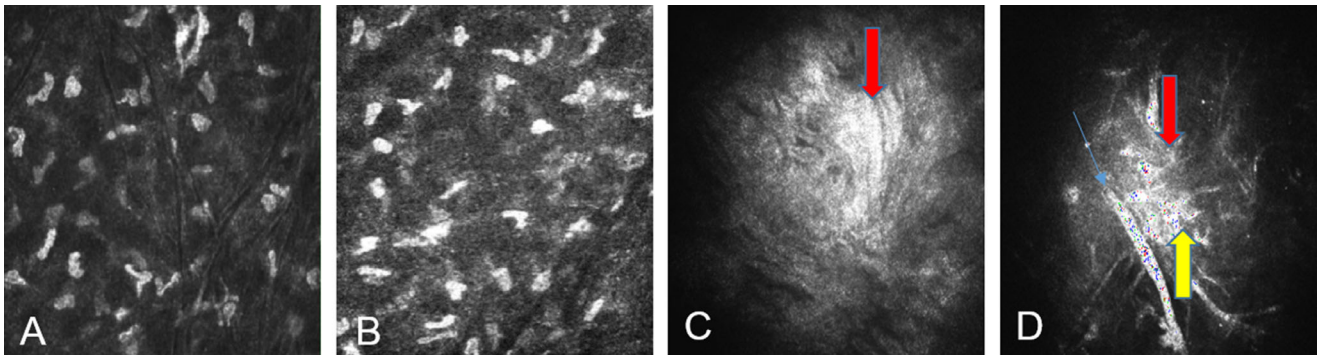

Figure 9. Cell count of the anterior and posterior corneal stroma for case 10 from G-3 12 months after the operation. (**A**) Anterior corneal stroma with abundant corneal stroma cells in a female patient 12 months after surgery. The number and morphology of corneal stroma cells are very similar to those of a normal stroma. (**B**) Posterior corneal stroma with a high number of corneal stroma cells for the same patient 12 months after surgery. The image shows that corneal stroma cells of the posterior stroma are similar in number and morphology to stromal cells of a normal cornea. (**C**) Presence of hyperreflective deposits (red arrow) corresponded with the preoperative paracentral corneal scarring observed in preoperative case 2 from G-1. (**D**) Improvement of the fibrotic tissue (red arrow) at the same level with the same case 2 from G-1 is observed. Note the presence of fibroblast (yellow arrow). Part of the superficial corneal nerve can be noted (blue arrow).

Patients Implanted with Recellularized Corneal Laminas (G-3)

Morphological Results. Unlike the decellularized laminas (G-2), which were mainly acellular (Fig. 5A), few ADASCs were seen in G-3 at 1 month after surgery. They were smaller than normal keratocytes on the anterior lamina surface (Fig. 6A), but they were more evident and similar to those on the posterior surface (Fig. 6B). At the same time, we also noticed that these cells were distributed in clusters (Figs. 6A, 6B). These clusters of mesenchymal cells dispersed over time until obtaining a geometrical distribution similar to that of normal corneal stroma (Figs. 6C–6E). In addition, the recellularized laminas consistently contained a higher number of keratocytes than the decellularized ones when observed 1 to 12 months after surgery (Fig. 8),[16] with some of them presenting dendritic shapes (Figs. 6C–6E).

Cell Density Results. One month after surgery, we observed only a few cells: a mean of 76 cells/mm^2 on the anterior surface of the lamina, 45 cells/mm^2 within the lamina, and 96 cells/mm^2 on the posterior surface of the lamina (Fig. 8). At 3 and 6 months, the cell density increased gradually over time (Fig. 8). Twelve months after implantation, the increase in cellular density on the recellularized anterior surface, posterior surface, and mid-lamina was statistically significant ($P < 0.001$) with respect to the first month after surgery (Figs. 6C, 6D, 8).

One year after surgery, the cellularity of the anterior and posterior corneal stroma showed a significantly higher number of keratocytes,[16] similar to that found in a normal cornea (Figs. 9A, 9B). Cell density on the anterior stroma ($P < 0.001$) and posterior stroma ($P < 0.001$) showed a statistically significant increase in the number of keratocytes with respect to the preoperative values (Figs. 7A, 7C).

Morphological Result of Fibrotic Tissue

We observed an absence of fibrotic tissue for cases 1 and 4 from G-1. We detected the presence of a few fibrotic tissues at 3 months after surgery in cases 2 and 3 and then observed full recovery of the corneal stroma during follow-up. Hyperreflective deposits that were observed corresponded with paracentral corneal scarring in preoperative case 2. Nevertheless, this scarring improved over the following months (Figs. 9C, 9D; Table 1).[14–16]

Table 1. Presence or Absence of Fibrotic Tissue in Groups 1, 2, and 3

Case	Group	Months				
		0	1	3	6	12
1	1	–	–	–	–	–
2	1	+++*	++*	++*	+*	+*
3	1	–	–	+†	–	–
4	1	–	–	+†	–	–
5	2	–	–	+/++†	+/++†	+/++
6	2	–	–	–	+/++†	+/++†
7	2	–	–	–	+/++†	+/++/+++†
8	2	–	+†	+/+++†	+/++†	–
9	2	–	+†	+/++†	+/++†	+/++†
10	3	–	+†	+/++†	+/++/+++†	+†
11	3	+++*	++†	+++†	+/++/+++†	+/++†
			+++*	+++*	++*	+*
12	3	–	–	–	+/++/+++†	+/++/+++†
13	3	–	–	+/++†	+/++/+++†	+/++†

Note: +, minor fibrotic tissue; ++, moderate fibrotic tissue; +++, high fibrotic tissue; –, absence of fibrotic tissue.

* Presence of paracentral scar with fibrotic tissue in the preoperative period; we observed an improvement of scars and decrease of fibrosis.

† Presence of fibrotic tissue during the postoperative follow-up.

The presence of fibrotic tissue in G-2 was observed beginning with the first postoperative month in cases 8 and 9, in the third month in case 5, and in the sixth month in cases 6 and 7. All detected fibrotic tissue corresponded to the paracentral corneal decellularized implanted laminas. However, at 12 months after surgery, we noted an absence of fibrotic tissue in case 8 (Table 1).

In G-3, we detected the presence of preoperative fibrotic tissue corresponding with the paracentral cornea scar in the anterior stroma in case 11. We observed the presence of postoperative fibrotic tissue at the first month in cases 10 and 11, as well as in case 13 beginning at the third month and in case 12 beginning at the sixth month. From 6 to 12 months,

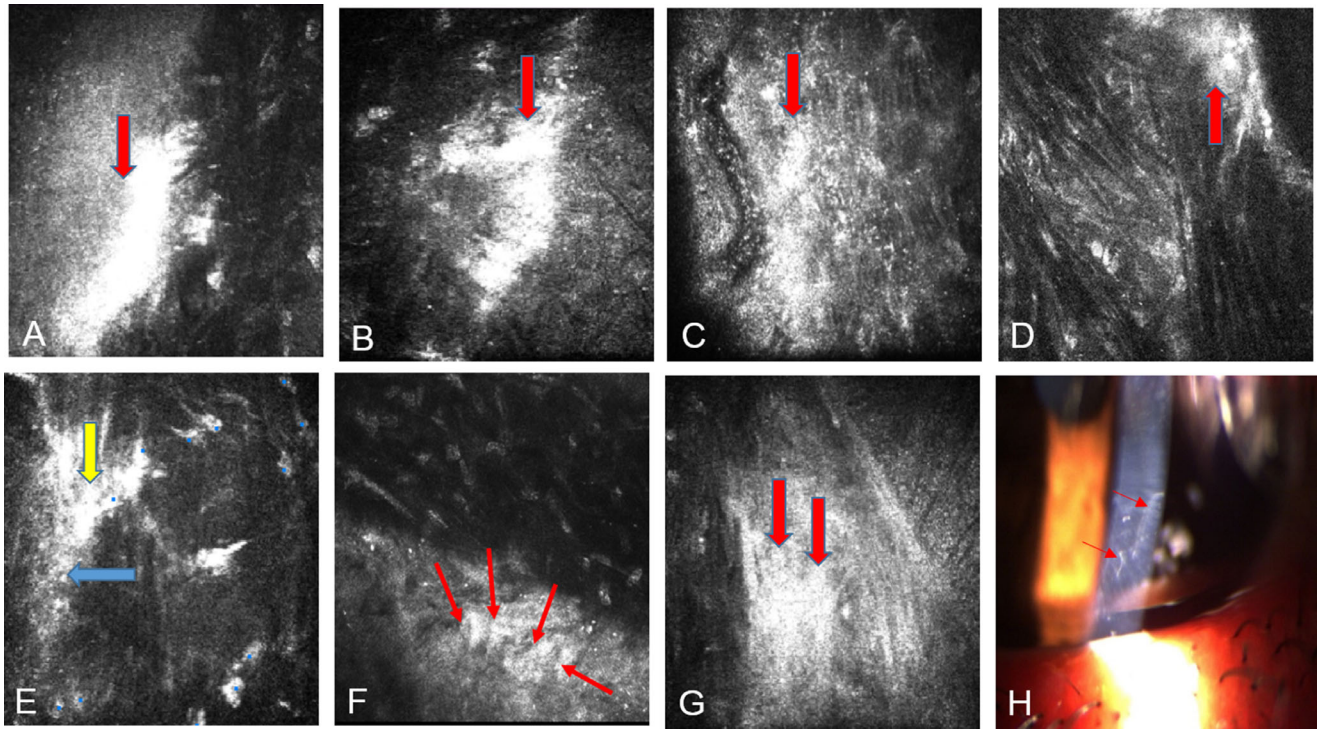

Figure 10. (**A**) The presence of highly reflective fibrotic tissue (red arrow) of keratoconic case 11 corresponds with the preoperative paracentral anterior stroma scar observed at 3 months after surgery. (**B**) The presence of fibrotic tissue (red arrow) is highly reflective on the periphery of the posterior surface of the lamina at 3 months for the same case. (**C**) Improvement of the paracentral preoperative fibrotic tissue (red arrow) on the anterior stroma of the same keratoconic case 6 months after the operation. (**D**) Improvement of the fibrotic tissue (red arrow) on the periphery of the posterior surface of the recellularized lamina of the same keratoconic case 12 months after surgery. (**E**) Presence of fibroblast or myofibroblast (yellow arrow) and fibrotic tissue (blue arrow) on the posterior surface of the decellularized lamina of a keratoconic patient 3 months after surgery. (**F**) Transition zone between the posterior surface of the decellularized lamina and the host stroma showing a number of migrating corneal stroma cells (possibly keratocytes?) with dendritical shapes (marked with red arrows) in a keratoconic patient 12 months after surgery. (**G**) Presence of highly reflective fibrotic tissue (red arrow) on the periphery in the mid-stroma of the decellularized lamina of a keratoconic patient 6 months after surgery. (**H**) Slit-lamp image of a keratoconic patient demonstrating peripheral scar tissue 6 months after surgery.

a decrease in fibrosis was noted in case 11 in the paracentral preoperative scar. In addition, we detected an improvement in postoperative fibrosis in most of the cases of this group (Figs. 10A–10D; Table 1).

In our study, the association between the degree of fibrosis and recellularization was evaluated through cumulative linked ordinal models to determine whether the coefficient associated with the independent variable (number of keratocytes densities) was statistically significant. However, we did not find a direct and significant association between recellularization and the presence of fibrotic tissue on the periphery of the decellularized or recellularized laminas. In G-2, *P* values obtained in the periphery of the anterior, middle, and posterior surfaces of the laminas were 0.823, 0.218, and 0.567, respectively. In G-3, *P* values obtained in the middle and posterior surfaces of the laminas were 0.505 and 0.123, respectively. On the periphery of the anterior surface of the laminas, we observed few occurrences of fibrotic tissue; thus, we have not obtained convergent results.

Comparison of Results Among the Three Groups

In our study, density was expressed as the number of cells/mm^2. Comparing the results obtained 12 months after surgery with preoperative conditions, the number of keratocytes increased (1) in the anterior stroma (ratios values 1.850, 1.857, and 1.853 in G-1, G-2, and G-3, respectively); (2) in the mid-stroma (ratio value 1.693 in G-1); and (3) in the posterior stroma (ratio values 2.048, 2.051, and 2.050 in G-1, G-2, and G-3, respectively) (Fig. 7; Table 2). We showed that the cell keratocyte densities in posterior stroma were higher in all of our groups than the normal keratocytes densities obtained in previous studies (408, 396, and 379 cells/mm^2) but lower than those found for the anterior stroma (430, 403, and 372 cells/mm^2) in all the cases, as well as in in the mid-stroma in G-1 (393 cells/mm^2) (Fig. 7).[4,14–16]

Twelve months after surgery, we observed in the anterior stroma a statistically significant difference ($P = 0.025$) in cell density among the three groups, with G3 having the highest cell density followed by G2 and then G1. However, in the posterior stroma, this difference in cell density among the groups was not statistically significant ($P = 0.311$) (Figs. 7A, 7C).

In addition, the anterior surface cell densities of the recellularized laminas in G-3 were statistically significant higher than in G-2 12 months after surgery ($P = 0.011$). Equivalent results in cellular densities were found in the mid-stroma of the laminas ($P = 0.011$), and a similar result was found for the posterior surface cellular density of the laminas ($P = 0.029$) (Fig. 8).

Table 2. Counted Nucleus Cell Ratios

Group	Anterior Stroma	Mid-Stroma	Posterior Stroma	Anterior Surface of the Lamina	Within the Lamina	Posterior Surface of the Lamina
1	372/201 = 1.850	393/232 = 1.693	379/185 = 2.048	—	—	—
2	403/217 = 1.857	—	396/193 = 2.051	102/28 = 3.642	95/14 = 6.785	165/43 = 3.837
3	430/232 = 1.853	—	408/199 = 2.050	251/69 = 3.637	254/38 = 6.684	328/86 = 3.813

Counted nucleus cell ratios are the proportion of cell densities 12 months after surgery compared with the preoperative values in groups 1, 2, and 3.

Discussion

In this innovative clinical study, we used confocal microscopy to observe the evolution of implanted mesenchymal stem cells with the aim of applying corneal regeneration as a new keratoconus therapy utilizing ADASCs. The results reported here complete the previous clinical results published elsewhere concerning this human clinical study.[14–16]

According to the results of this confocal study, following the injection of only ADASCs into corneal pockets created using a femtosecond laser in G-1 there was a statistically significant increase in the density of corneal keratocytes in the anterior, mid-, and posterior stroma ($P < 0.001$). This correlates well with the already reported production of new collagen, which resulted in an improved corneal thickness.[14] We also observed in G-1 relevant changes in the morphology of the implanted cells from the moment of their implantation into the corneal pockets, as the morphology of the ADASCs was round in shape until the third month. This finding suggests survival of the implanted stem cells following their implantation. Later on, the cells showed changes ranging from forming clusters around individual cells to developing the confocal appearance of adult stromal corneal cells at the 12 months after surgery.

In G-2 and G-3, where corneal laminas were implanted with or without impregnation with ADASCs, we observed that implantation of such laminas, whether or not colonized by ADASCs, favored an increase in the number of corneal stromal cells in the anterior and posterior stroma of the cornea in a highly statistically significant level ($P < 0.001$) (Figs. 7A, 7C).

In vivo confocal microscopy offers the possibility of studying the normal morphology of the cornea and microstructural changes that can occur in keratocyte density and in the morphology of keratocytes in keratoconic cornea.[4,7,11,20,21,22] Normal human keratocytes in full-thickness central corneas have been studied by various authors[21,22] using a different technology (Tandem Scanning Corporation, Reston, VA, USA) and different metrics (cells/mm^3) with confocal microscopes. Other authors in more recent publications used a laser scanning in vivo confocal microscope (Heidelberg Retina Tomograph II/RCM) and found that mean keratocyte density in the control group was 786 ± 244 cells/mm^2 in the anterior stroma and 293 ± 35 cells/mm^2 in the posterior stroma. In the keratoconus group that did not wear contact lenses, the values were 662 ± 193 cells/mm^2 and 236 ± 32.6 cells/mm^2 in the anterior and posterior stroma, respectively.[4]

In our study, we increased cell densities in the anterior mid- and posterior stroma at 12 months compared to the preoperative level (Figs. 7A–7C; Table 2), but we did not detect any new formation of fibrotic structures (Figs. 9A, 9B). The presence of fibrotic tissue seemed to be related to groups that received only laminas (with or without ADASCs). This was more evident in G-3, whereas in G-1 there was an absence of fibrotic structures until 12 months after surgery. We noticed an improvement of corneal scarring for case 2 from G-1 at 12 months after surgery (Figs. 9C, 9D; Table 1).[14–16] Nevertheless, in G-2 and G-3 fibrotic structures were present in patients almost in the periphery of the implanted laminas (Table 1). It has been postulated that mesenchymal stem cells can either avoid or improve preexisting scars (Figs. 9C, 9D, 10A, 10C), although, in the non-peripheral areas of the implanted laminas, we did not observe differences in corneal transparency among the three groups, nor did we observe cornea haze.[14–16]

Moreover, changes inside the acellular laminas implanted in G-2 were also observed. This finding demonstrates that the decellularized lamina was colonized by the patient's own keratocytes, a process that began in the first month. After 12 months, the lamina was found to be completely recellularized (Fig. 8).

On the other hand, we have also observed that, from the first postoperative month in the recellularized laminas of G-3, a decrease occurred in the clusters of the mesenchymal cells implanted on the laminas. Such cellular morphological changes were clearly seen to occur first on the posterior surface followed by the anterior surface, and the number of cells statistically and significantly increased from 1 month after the surgery to 12 months after surgery. This finding may suggest survival and differentiation of the implanted cells toward keratocytes and/or repopulation of these laminas, with migration of the host corneal stromal keratocytes being stimulated to proliferate toward the decellularized corneal tissue.[23] Obviously, as the cells could not be labeled before implantation due to possible interference with transparency and hence ethical issues, the distinction between both populations is not possible. This finding correlates well with another report[23] that demonstrated that propagation and migration of corneal fibroblasts happens in parallel with furrow ridges aligned with collagen lamellae. During the migration of these cells, tracks for propagation are established by alignment of the fibrils through the generation of a mechanical force. It is also possible that chemoattractant factors may be released by the ADASCs during the evolution following implantation.[24]

In addition, we observed in this study that stromal cells, which are likely to be keratocytes, fibroblasts, or myofibroblasts, have migrated from the corneal stroma toward the edge of the lamina in cases where no cells were injected (Figs. 10E, 10F). Such stromal cells (keratocytes) show peripheral prolongations and morphological transformations with dendritic forms, indicating that they have differentiated into fibroblasts and myofibroblasts during their period of activity and that they are capable of sliding

on the collagen fibers of the decellularized tissue (Figs. 10E, 10F).[23] We also observed, up to 12 months after surgery, the development of paracentral fibrotic tissue on top of the photoablated stroma of the implanted tissue (Figs. 10B, 10D, 10E, 10G, 10H).[23]

We have reported herein an evolution in morphology of corneal stromal cells, presumed to be keratocytes. It has been reported that these cells are normally oval and irregular in shape and without a dendritic shape. It is when they migrate or are activated that they assume a dendritic shape.[22,23] Because the evolution of stromal cell morphology in our study did not follow such a pattern, our observation does not support previous reports,[17] which have described that in adult tissue keratocytes are mitotically quiescent and have a flat, dendritic morphology.[25] Furthermore, it would be important in future studies to establish differences among the various morphologies that are observed in stromal cells to compare the evolution of those that have a non-dendritic shape to those that have dendritic shape and the biological implications that such morphological changes may have.

A relevant issue of the present study is the methodology used for counting stromal cells, which was a specific manual method. This may introduce a certain amount of subjectivity and interpretation bias; however, this method provided us with a more accurate and discriminating cell count than the automated cell counts of the microscope, which are affected by large variability, inaccuracies, and misinterpretations (Fig. 3). The presence of highly reflective fibrotic tissue in the studied areas could make it difficult to discriminate the edges of the keratocytes nuclei that were the main focus of our study (Figs. 9C, 9D, 10).

We believe that it is necessary to establish a more objective cell count method based on image processing programs and specific algorithms in which the contrast and illumination can be edited and various specialized filters used to optimize visualization of keratocytes cells and to better calculate their size.

In conclusion, confocal corneal microscopy combined with the technology used in our investigation has shown to be a very efficient tool for in vivo assessment and follow-up of corneas implanted with mesenchymal stem cells for corneal regeneration purposes. We have reported the confocal microscopy outcomes after implantation of ADASCs in the selected surgical plane, which allowed qualitative and quantitative assessment of them during the experiment. Moreover, confocal corneal microscopy allowed monitoring of the progressive morphological changes that occurred in the decellularized and recellularized laminas throughout the observation period and assisted in determining changes in cell densities in the grafted tissue, as well as in all the corneal stroma.

Stromal cells are significantly increased at the level of implantation when they are injected into the corneal stroma (Fig. 7B). In addition, they induce a significant increase in the level of stromal cells when implanted jointly with a corneal lamina impregnated at the surface with ADASCs. This increase is larger than that observed when acellular corneal laminas are implanted (Figs. 7A, 7C), even when the implantation is followed by repopulation of the acellular lamina by the resident stromal cells (Fig. 8). Whether these findings indicate survival of the mesenchymal ADASCs and their differentiation into keratocytes or that such mesenchymal cells cause a biological stimulus for the proliferation of the resident cells has yet to be confirmed in future studies.

Acknowledgments

The authors thank Eric Bangert and Heidelberg Engineering for the generous temporary donation of the confocal microscopy and confocal software analysis software used for this investigation; Marc Assouwad from Laser Vision for her assistance in the logistics of the study; Albert Aazar and Reviva Regenerative for administrative management of the laboratory; and Ibrahim Achkar, who was responsible for the liposuction and adipose tissue management until the moment of the laboratory study.

Supported by Optica General, Saida Lebanon, and the Vissum Ophthalmological Institute of Alicante, Spain; by the Red Temática de Investigación Cooperativa en Salud (RD16/0008/0012); by the Instituto Carlos III–General Subdirection of Networks and Cooperative Investigation Centers (R&D&I National Plan 2008-2011); by the European Regional Development Fund; and by a Roche Farma SA grant (MPdM).

Disclosure: **M. El Zarif**, None; **K.A. Jawad**, None; **J.L. Alió Del Barrio**, CSO (C); **Z.A. Jawad**, None; **A. Palazón-Bru**, None; **M.P. de Miguel**, Roche Farma SA (F); **P. Saba**, None; **N. Makdissy**, None; **J.L. Alió**, AkkoLens (C, R), Blue Green Company (F), Carl Zeiss Meditec (C, R), CSO (R), Dompé (R), Hanita Lenses (C, R), Jaypee Brothers (P), Maghrabi Hospital (C), Mediphacos (R), Oftalcare Nutravision (F), Omeros (C), Ophtec (F), Santen Pharmaceutical (C, F, R), Oculentis (C, R), Presbia (C), Schwind eye-tech-solutions (F, R), Slack Incorporated (C), Topcon Medical Systems (C), VisiDome (F)

References

1. Sekundo W, Stevens JD. Surgical treatment of keratoconus at the turn of the 20th century. *J Refract Surg*. 2001;17:69–73.
2. Bechrakis N, Blom ML, Stark WJ, Green WR. Recurrent keratoconus. *Cornea*. 1994;13:73–77.
3. Pinero DP, Alió JL, Barraquer RI, et al. Corneal biomechanics, refraction, and corneal aberrometry in keratoconus: an integrated study. *Invest Ophthalmol Vis Sci*. 2010;51:1948–1955.
4. Ku JY, Niederer RL, Patel DV, et al. Laser scanning in vivo confocal analysis of keratocyte density in keratoconus. *Ophthalmology*. 2008;115:845–850.
5. Sherwin T, Ismail S, Loh I, McGhee JJ. Histopathology (from keratoconus pathology to pathogenesis). In: Alió J , ed. *Keratoconus: Recent Advances in Diagnosis and Treatment (Essentials in Ophthalmology)*. Cham, Switzerland: Springer; 2017:25–41.
6. Alió JL, Pinero DP, Aleson A, et al. Keratoconus-integrated characterization considering anterior corneal aberrations, internal astigmatism, and corneal biomechanics. *J Cataract Refract Surg*. 2011;37:552–568.
7. Mastropasqua L, Nubile M. *Confocal Microscopy of the Cornea*. Thorofare, NJ: Slack; 2002;7–16.
8. Ali Javadi M, Kanavi MR, Mahdavi M, et al. Comparison of keratocyte density between keratoconus, post-laser in situ keratomileusis keratectasia, and uncomplicated post-laser in situ keratomileusis cases. A confocal scan study. *Cornea*. 2009;28:774–779.
9. Edmund C. Assessment of an elastic model in the pathogenesis of keratoconus. *Acta Ophthalmol (Copenh)*. 1987;65:545–550.
10. Fournié P, Galiacy SD, Malecaze F. Modern pathogenesis of keratoconus: genomics and proteomics. In: Alió JL, ed. *Keratoconus: Recent Advances in Diagnosis and Treatment (Essentials in Ophthalmology)*. Cham, Switzerland: Springer; 2017;7–12.

11. Mastropasqua L, Nubile M. *Confocal Microscopy of the Cornea*. Thorofare, NJ: Slack; 2002;38–44.
12. Watts A, Colby K. Contact lenses for keratoconus. In: Alió J , ed. *Keratoconus: Recent Advances in Diagnosis and Treatment (Essentials in Ophthalmology)*. Cham, Switzerland: Springer; 2017:187–194.
13. Arnalich-Montiel F, Alio Del Barrio JL, Alio JL. Corneal surgery in keratoconus: which type, which technique, which outcomes? *Eye Vis (Lond)*. 2016;3:2.
14. Alió Del Barrio JL, El Zarif M, de Miguel MP, et al. Cellular therapy with human autologous adipose-derived adult stem cells for advanced keratoconus. *Cornea*. 2017;36:952–960.
15. Alió Del Barrio JL, El Zarif M, Azaar A, et al. Corneal stroma enhancement with decellularized stromal laminas with or without stem cell recellularization for advanced keratoconus. *Am J Ophthalmol*. 2018;186:47–58.
16. Alió JL, Alió Del Barrio JL, El Zarif M, et al. Regenerative surgery of the corneal stroma for advanced keratoconus: one year outcomes. *Am J Ophthalmol*. 2019;203:53–68.
17. Arnalich-Montiel F, Pastor S, Blazquez-Martinez A, et al. Adipose-derived stem cells are a source for cell therapy of the corneal stroma. *Stem Cells*. 2008;26:570–579.
18. Du Y, Carlson EC, Funderburgh ML, et al. Stem cell therapy restores transparency to defective murine corneas. *Stem Cells*. 2009;27:1635–1642.
19. Liu H, Zhang J, Liu CY, et al. Cell therapy of congenital corneal diseases with umbilical mesenchymal stem cells: lumican null mice. *PLoS One*. 2010;5:e10707.
20. Guthoff R, Klink T, Schlunck G, Grehn F. Die sickerkissenuntersuchung mittels konfokaler in-vivo mikroskopie mit dem rostocker cornea modul - erste erfahrungen. *Klin Monatsbl Augenheilkd*. 2005;222:R8.
21. Patel S, McLaren J, Hodge D, Bourne W. Normal human keratocyte density and corneal thickness measurement by using confocal microscopy in vivo. *Invest Ophthalmol Vis Sci*. 2001;42:333–339.
22. Erie JC, Patel SV, McLaren JW, et al. Keratocyte density in keratoconus. A confocal microscopy study(a). *Am J Ophthalmol*. 2002;134:689–695.
23. Petroll WM, Kivanany PB, Hagenasr D, Graham EK. Corneal fibroblast migration patterns during intrastromal wound healing correlate with ECM structure and alignment. *Invest Ophthalmol Vis Sci*. 2015;56:7352–7361.
24. Phinney DG, Prockop DJ. Concise review: mesenchymal stem/multipotent stromal cells: the state of transdifferentiation and modes of tissue repair–current views. *Stem Cells*. 2007;25:2896–2902.
25. Jester JV, Moller-Pedersen T, Huang J, et al. The cellular basis of corneal transparency: evidence for 'corneal crystallins'. *J Cell Sci*. 1999;112:613–622.

Investigative Ophthalmology & Visual Science